Published in final edited form as:
Vasc Med. 2011 April ; 16(2): 145–156. doi:10.1177/1358863X10392474.

Emerging diagnostic and therapeutic molecular imaging applications in vascular disease

Luis H Eraso[1,2], **Muredach P Reilly**[1,2,3], **Chandra Sehgal**[3,4], and **Emile R Mohler III**[1,2,3]

[1]Cardiovascular Division, Vascular Medicine Section, University of Pennsylvania School of Medicine, Philadelphia, PA, USA

[2]Cardiovascular Institute, University of Pennsylvania School of Medicine, Philadelphia, PA, USA

[3]The Institute for the Translational Medicine and Therapeutics (ITMAT), University of Pennsylvania School of Medicine, Philadelphia, PA, USA

[4]Ultrasound Research Laboratory, Department of Radiology, University of Pennsylvania School of Medicine, Philadelphia, PA, USA

Abstract

Assessment of vascular disease has evolved from mere indirect and direct measurements of luminal stenosis to sophisticated imaging methods to depict millimeter structural changes of the vasculature. In the near future, the emergence of multimodal molecular imaging strategies may enable robust therapeutic and diagnostic (‘theragnostic’) approaches to vascular diseases that comprehensively consider structural, functional, biological and genomic characteristics of the disease in individualized risk assessment, early diagnosis and delivery of targeted interventions. This review presents a summary of recent preclinical and clinical developments in molecular imaging and theragnostic applications covering diverse atherosclerosis events such as endothelial activation, macrophage infammatory activity, plaque neovascularization and arterial thrombosis. The main focus is on molecular targets designed for imaging platforms commonly used in clinical medicine including magnetic resonance, computed tomography and positron emission tomography. A special emphasis is given to vascular ultrasound applications, considering the important role this imaging platform plays in the clinical and research practice of the vascular medicine specialty.

Keywords

atherosclerosis plaque; imaging based therapeutic delivery systems; molecular imaging; theragnostics; thrombosis; vascular ultrasound

Introduction

Despite significant diagnostic and therapeutic advances achieved in the last few decades, atherosclerosis still is one of the leading causes of morbidity and mortality worldwide. Until recently, the hemodynamic characteristics of the lesion prevailed over other aspects of the atherosclerosis pathobiologic process. However, it is now well established that independent of the degree of stenosis, other characteristics of the atherosclerosis process, such as

Corresponding authors: Luis H Eraso and Emile Mohler III, Cardiovascular Division, Vascular Medicine Section University of Pennsylvania, 6th Penn Tower, 3400 Spruce Street, Philadelphia, PA 19104, USA, Luis.Eraso@uphs.upenn.edu, Mohler@uphs.upenn.edu.

endothelial dysfunction, plaque inflammatory activity, platelet agreeability and neo-vascularization, are important to determine the progression and complications of the human atherosclerosis plaque.

With this backdrop, it is paramount that critical events in the atherosclerosis processes are imaged at the molecular level, even before a flow-limiting lesion develops. In atherosclerosis and other vascular diseases, molecular imaging provides a personalized insight of the disease-specific biological events, enables novel non-invasive strategies for individualized risk assessment, and facilitates monitoring of highly targeted thera-pies.[1] Moreover, new imaging technologies targeting specific vascular receptors and development of site-specific delivery methods have expanded the molecular imaging spectrum from a lone diagnostic tool to a mode of therapeutic intervention. In this context, theragnostics, defined as the fusion of diagnosis and therapeutics,[2] is well exemplified by emerging vascular imaging modalities in which highly specific and personalized interventions are delivered using structural, functional, and genomic expressions of the disease.[3,4]

Molecular imaging is a rapidly developing discipline aimed at depicting cellular and sub-cellular processes using traditional and novel imaging platforms.[1] In contrast to developments in cancer diagnosis, the use of molecular imaging in atherosclerosis and other vascular diseases has evolved at a slower pace mainly due to a smaller and highly heterogeneous biologic substrate. However, recent advances in the design of imaging enhancement agents, sophisticated multimodal imaging systems (i.e. ultrasound, MRI [magnetic resonance imaging], CT [computed tomography], PET [positron emission tomography]) and the advent of novel imaging platforms suggest the evaluation of vascular disease has entered a new era.

Acknowledging some important molecular imaging and theragnostic strategies may be overlooked in this review – we aimed to focus our synopsis by selecting molecular imaging modalities based on the following criteria. First, the review was limited to applications designed for imaging platforms currently used in clinical medicine (i.e. ultrasound, MRI, PET/CT [positron emission tomography co-registration with computer tomography]) with special emphasis given to applications designed for vascular ultrasound, an imaging platform particularly important to contemporary vascular medicine clinical and research practice. Second, we gave priority to examples in each imaging modality in which extensive clinical information exists, such as ultrasound vasa vasorum (VV) imaging, macrophage activity imaging with super-magnetic particles and radiopharmaceuticals, and ultrasound-enhanced thrombolysis (UET) in the therapeutic section.

Molecular imaging assessment of the atherosclerosis plaque

Atherosclerosis formation and progression involve multiple pathobiologic processes occurring at different stages in multiple vascular territories. Designing atherosclerosis molecular imaging probes and choosing the ideal imaging platform (e.g. MRI, CT-SPECT [computer tomography-single photon emission computed tomography] or ultrasound) requires a comprehensive understanding of the heterogeneous atherosclerosis process and its multiple functional components.

The response-to-retention model of atherogenesis assumes that the seminal event is retention of Apo-B lipoproteins in the subendothelium.[5,6] This critical initiation event leads to local and systemic inflammatory signaling mediated by chemokines and cytokines,[7] and expression of endothelial cell adhesion molecules including vascular cell adhesion molecule-1 (VCAM-1), intercellular adhesion molecule-1 (ICAM-1), and P-selectin by the activated endothelium.[8] The primary role of endothelial activation is to orchestrate a rapid defense and repair response to any given insult. However, in the setting of sustained

hypercholesterolemia and other triggers of endothelial activation (e.g. platelet-mediated endothelial activation via Ib and IIb/IIIa surface glycoprotiens[9,10]), rolling monocytes and T-lymphocytes adhere to the vascular wall and then migrate to the intima.[11] In the sub-endothelium, monocytes differentiate into macrophages which accumulate modified low-density lipoprotein via scavenger receptors and pattern recognition receptors such as CD68, CD36, SR-A and TLR4.[12,13] Macrophages are not only important in the development of foam cells predominant in the fatty streak and enlargement of the extracellular lipid core,[14] but also contribute to the thinning of the fibrous cap observed in vulnerable plaque via secretion of matrix metalloproteases (MMPs) and other inflammatory molecules abundant in the rupture-prone plaques.[15–17]

Molecular imaging applications designed for ultrasound, MRI and PET/CT individually capture only limited aspects of the vast spectrum of pathobiologic events involved in atherosclerosis development and progression. Therefore, based on their unique advantages and disadvantages, these molecular imaging applications may have a complementary, rather than a competitive, role in depicting the molecular underpinnings of atherosclerosis, as illustrated in Figure 1.

Ultrasound-based molecular imaging applications in atherosclerosis

The clinical experience of using ultrasound contrast in clinical echocardiography combined with recent advances in molecular biology technologies has broadened the spectrum of vascular ultrasound. Novel applications based on the use of contrast ultrasound enhancement, such as direct visualization of arterial VV[18] or early endothelial inflammatory response assessment with targeted ultrasound agents,[19] are promising examples that ultrasound could be a high-resolution and high-sensitivity imaging technique ideally suited to depict real-time molecular processes.

Gramiak and Shah first described the use of agitated saline to enhance the contour of the aorta and heart chambers more than 30 years ago.[20] Modern ultrasound contrast agents (UCAs) are gas-filled molecules (usually referred to as microbubbles) that have an outer shell composed of phospholipids, liposomes or other biodegradable polymers. The elastic properties of the shell material and the gas content of the microbubble define the acoustic response, the stability and the effective imaging time. The other important structural component of the microbubbles is the gas core. Late generation UCAs are usually filled with high molecular mass gases (e.g. octafluoropropane, sulfur hexafluoride or perfluorohexane) that provide greater stability, improved acoustic response and enable longer imaging times when compared to earlier air-filled microbubbles.

Microbubbles have many properties that make them ideal for ultrasound contrast enhancement and molecular imaging of the vasculature. They have a molecular size (1–5 μm) similar to mature red blood cells, conferring them a comparable rheologic behavior.[21] They are strict intra-vascular tracers with no significant retention in the diseased tissue unless selective molecular targeting is induced by changes in the structure of the shell or molecular probes are conjugated in the outer shell. Their physical and ultrasonic characteristics enable them to be specifically differentiated from surrounding tissues. Namely, microbubbles tend to undergo volumetric oscillation, providing a greater ability to reflect, absorb and re-radiate sound energy. In addition, they have a high compressibility difference with surrounding tissues (acoustic impedance) in response to the pressure amplitude from the external ultrasound wave.

The pressure amplitude, also referred to as the acoustic power or output power of the scanner, is usually measured as the mechanical index (MI). At a low MI (< 0.25), microbubbles tend to undergo linear oscillation with an equal compression and rarefaction

(expansion) amplitude, resulting in limited contrast enhancement. At a higher MI (0.2–0.7), microbubbles have a non-linear volumetric oscillation with a higher difference between rarefaction and compression, resulting in an optimal contrast enhancement. At this non-linear oscillation pattern, microbubbles re-radiate a sound field containing a specific harmonic spectrum easily distinguished from surrounding tissues which usually contain a smaller proportion of harmonics.[22,23] At a high MI (0.8 or higher), microbubble destruction occurs, generating a high-intensity signal often referred to as a 'stimulated acoustic emission'. This high-intensity signal has been used to measure and depict microvascular flow using video intensity curves in various tissues including the myocardium, skeletal muscle, kidneys and the periadventia of large vessels.[24–27] Once the microbubbles are destroyed, the shell is metabolized, the gas is dissolved in surrounding fluids, or if a non-dissolvable gas is used, smaller fragments are exhaled during capillary lung transit. For a more comprehensive review of the principles of contrast-enhanced ultrasound imaging and therapy we encourage readers to review the papers by Stride,[28] Voigt,[29] and Miller et al.[30]

The Federal Drug Administration (FDA) currently approves the use of UCAs only in clinical echocardiography primarily for opacification of the left ventricle and to improve delineation of the endocardial border. Anecdotal reports of serious adverse events, including death, prompted the FDA to limit the use of UCAs to subjects without clinical evidence of decompensated heart failure, pulmonary hypertension or right-to-left intra-cardiac shunts. However, recently published large prospective[31] and retrospective studies[32] support the concept that contrast enhancement in ultrasound is safe and reliable. In a recent prospective study of 26,774 subjects, the use of contrast ultrasound agents used to perform stress echocardiography was not associated with an increased cardiovascular mortality or morbidity.[33] Another large, multicenter, retrospective analysis of 66,164 doses of ultrasound contrast agents over a 4.5-year period revealed that the incidence of major adverse reactions after using microbubbles as a cardiovascular contrast agent is similar or even lower than the incidence of adverse events reported after using contrast agents in other imaging modalities (e.g. CT angiogram (CTA) and MRI).[32] Even if all reported events are attributed to the use of UCAs, the risk of death would be significantly low (1:500,000) and no greater than performing an echocardiogram without contrast enhancement.[34]

The use of UCAs beyond clinical echocardiography is not yet approved by the FDA. However, the extensive safety background information collected from human translational research studies evaluating microvascular flow in non-cardiac organ systems[30,35,36] and thousands of contrast-enhanced echocardiograms performed daily in the United States suggest regulatory approval to use UCAs in other vascular conditions is feasible in the near future once disease-specific and more robust safety information is collected. Imaging of non-cardiac vasculature can be achieved with a lower contrast dose, lower MI and limited acoustic energy exposure to the heart and pulmonary vasculature.[27]

Ultrasound-enhanced imaging of intra-plaque neovascularization

The VV is a network of small blood vessels that supply oxygen and other blood nutrients to the walls of large arteries. Several animal model systems and human observational studies substantiate the hypothesis that disruptive changes in the regulation of the periadventitial vasculature may have an active role in atherosclerosis development and progression.[37–39] Early atherosclerosis is accompanied by significant hyperplasia of the VV and disruptive neovascularization of the media and intima even before endothelial dysfunction occurs, suggesting this phenomenon is a seminal event in atherosclerosis initiation and progression.[39,40] At later stages, plaque neovascularization correlates with hemorrhage and rupture. Autocrine and systemic factors influence arterial wall disruptive neovascularization throughout the entire spectrum of the atherosclerosis process.[38] Ectopic neovascularization

is also thought to be a maladaptive response to the increased nutritional demand[37] and cellular hypoxia stimulus from the atheromatous plaque. Notably, cellular hypoxia within atherosclerosis plaque is associated with an increased expression of macrophages, CD8, proangiogenic factors and hypoxia inducible factor (HIF).[41] Experimental models of plaque neovascularization demonstrate that contrast-enhanced ultrasound and other non-invasive imaging strategies such as microscopic three-dimensional (3D) CT and contrast-enhanced magnetic resonance (CMR) could be used to image plaque neovascularization.[38]

Contrast-enhanced ultrasound (CEU) in particular, is an accurate, low cost, non-invasive imaging method able to provide a real-time quantification and determination of the extent and structural characteristics of the periadventitial microvasculature and plaque neovascularization. CEU utility to portray VV hyperplasia has been demonstrated in several animal and clinical models.[40,42,44–46] In a Rapacz familial hypercholesterolemia swine model of atherosclerosis induced by mechanical vascular injury, Herrmann et al. used CEU imaging to demonstrate that the VV network development preceded endothelial dysfunction, and the neovascularization process progressed from no detectable microvessels at 5 weeks, to an extensive and diffuse periadventitial and ectopic neovascularization at 43 weeks.[40] Similarly, several clinical observational studies demonstrate the ability of contrast-enhanced ultrasound methods to depict periadventitial vasculature and intra-plaque neovascularization in patients with carotid atherosclerotic disease.[18,43–46] Giannoni et al. studied 77 subjects demonstrating that high-grade intra-plaque neovascularization was more frequent in symptomatic versus asymptomatic individuals (1/64 vs 9/9, respectively, $p < 0.001$). They also noted that contrast ultrasound enhancement of carotid plaque neovascularization correlated with the degree of microvascular density. Histological specimens from symptomatic subjects had a higher intensity of vascular endothelial growth factor (VEGF) and matrix metalloproteinase-3 (MMP3) immunostaining, and microvessesls in the periadventitial aspect of the plaque were smaller (Figure 2).[44] In a larger study ($n = 104$), Xiong et al. used a quantitative method (signal intensity) to demonstrate that periadventitial microvasculature and ectopic neovascularization was significantly higher in symptomatic patients when compared to asymptomatic individuals (13.9 ± 6.4 dB vs 8.8 ± 5.2 dB, $p < 0.001$).[24]

Targeted ultrasound agents for early atherosclerosis assessment

The use of targeted and acoustically active probes is a promising molecular imaging approach to depict endothelial activation and immune cell retention observed in early atherosclerosis.[47]

Some of the ultrasound contrast agents have an intrinsic affinity to detect early endothelial activation. Microbubble adherence to leucocytes that attach to the activated endothelium appears to be mediated by complement and may be enhanced by chemical changes induced in the microbubble lipid-shell, such as a negative charge in the phosphatidyl-serine component.[47,48] In a large animal atherosclerosis model of endothelial dysfunction induced by local arterial injury and hyperlipidemia, lipid-shell microbubble binding to the carotid artery-activated endothelium was directly visualized using high-magnification electron microscopy and high-frequency ultrasound (Figure 3).[49] Similarly, others have demonstrated that albumin-shell microbubbles have increased affinity for the β2-integrin Mac-1 leukocyte receptor.[47]

A more specific strategy for early atherosclerosis imaging is to perform selective targeting by incorporating, through direct conjugation or through an avidin/streptavidin biotinylation method, an antibody, glycoprotein, carbohydrate, peptide or any other disease-specific molecular target into the microbubble shell.[29,47,50] In a small animal model system, the

highest retention of VCAM-1-targeted microbubbles was observed in apolipoprotein E-deficient mice with severe atherosclerosis.[19] In larger animals, intra-vascular ultrasound imaging of the atheromatous-related endothelial abnormalities has been achieved using immunoliposomes tagged with antibodies directed against ICAM-1 and VCAM-1.[51] These studies provide proof-of-principle that real-time assessment of early atherosclerosis inflammation is feasible using targeting ultrasound contrast agents. However, low microbubble retention at the atherosclerosis site due to high-velocity and high-shear stress, and low specificity of selected targets suggest further research development is necessary before human translation is attempted.[31,47]

Atherosclerosis macrophage activity assessment using super-magnetic particles

Human atherosclerotic plaque inflammation has been demonstrated using magnetic resonance.[52] Notably, recent clinical trials with super-magnetic particles provide proof of the clinical feasibility of tracking macrophage infiltration of carotid atheroma as a surrogate marker of plaque inflammation and in risk assessment.[53,54]

Ultra-small superparamagnetic particles of iron oxide (USPIO) are large circulating iron oxide nanoparticles (ferumoxtran-10) cleared very slowly (24–36 hours) by the reticuloendothelial system, making them ideal for atherosclerosis and lymphatic vessel imaging. The principle of using USPIO in atherosclerosis relies on the similar molecular size (less than 50 nm) of these particles to oxidized low-density cholesterol (ox-LDL-c), their ability to be retained in the sub-endothelial space of dysfunctional endo-thelium[55] and their specific affinity for scavenger receptors and other outer cell membrane molecules expressed by activated macrophages, such as the integrin receptor Mac-1 (CD11b/CD18, αMβ2)[56] and phosphatidylserine.[57] The ideal visualization of USPIO particles with activated macrophages is achieved with a T2*-weighted gradient echo sequence in which areas of high plaque inflammatory activity are represented by a signal hypodensity (Figure 4).

In humans, there is extensive evidence that supports using USPIO imaging in the assessment of carotid atheroma macrophage infiltration and plaque vulnerability. Histopathological correlation shows that up to 75% of the ruptured or ruptured-prone lesions contain high concentrations of USPIO, whereas this agent was only present in 7% of the stable plaques.[52] In the ATHEROMA (Atorvastatin Therapy: Effects on Reduction Of Macrophage Activity) study, a prospective, randomized, double-blind trial of 47 subjects with clinically documented carotid atherosclerosis, subjects were randomly assigned to a low dose (10 mg) or high dose (80 mg) of atorvastatin once a day for 12 weeks. Subjects in the high-dose group had a significant reduction of macrophage activity at 6 and 12 weeks (Figure 4), whereas no reduction was noted in the low-dose group. Molecular imaging signaling was concordant with a significant LDL-c reduction (−29%, 95% CI −30% to −15%, $p < 0.0001$) and microemboli count reduction (−91%, 95% CI −97% to −78%, $p < 0.0001$) at 12 weeks.[54]

Evidence that macrophage activity assessment by MRI is a valid outcome to use in clinical trials is robust. However, as in most of the emerging molecular imaging strategies, future research is required to determine the ability of this imaging technique to predict long-term cardiovascular outcomes. Additional studies are also imperative to evaluate the long-term safety of using a molecule such as USPIO that can potentially increase atherosclerosis plaque iron content, particularly if recurrent exposure is required.[58] Some hypothesize that a local increase in the content of iron may promote oxidative stress and extracellular matrix degradation, paradoxically inducing atherosclerosis progression and plaque rupture.[59]

Other MRI probes also have been studied at the preclinical level to depict molecular characteristics of atherosclerotic lesions. Novel approaches tagging gadolinium and other magnetically active probes routinely used in clinical medicine with proteins involved in the endothelial dysfunction process include the use of Apo-A1 mimetic agents[60] and antibodies targeting oxidized-specific epitopes such as the human IK17 or the murine MDA2 and E06.[61]

Plaque inflammation and platelet activity using radiolabeled probes

In the last few years PET/CT has become a widely acceptable tool in oncology and clinical cardiology to depict cellular infiltration, ischemia and other disease-specific molecular process. In atherosclerosis imaging, recent developments based on the use of dedicated fusion imaging systems that combine PET imaging or single photon emission computed tomography (SPECT) with either CT or MRI[62] has enabled accurate anatomic and molecular correlation of the atherosclerotic disease process (Figure 5).[63]

Similar to super-magnetic particles, radiolabeled probes depict activated macrophages within atheromatous plaque, although in a different metabolic pathway. Cellular inflammatory activity is characterized by increased glucose turnover. Vulnerable plaques characteristically have a thin fibrous cap and sustained inflammatory activity that correlates with the number of activated macrophages.[15,64] Metabolically active macrophages have an increased glucose uptake that can be detected as an increased radioactivity using 2-[^{18}F]fluoro-2-deoxy-D-glucose positron emission tomography (^{18}F-[FDG]-PET).[65–67]

Yun et al. first reported the uptake of ^{18}F-[FDG] in atherosclerosis lesions of large arteries in humans.[68] Subsequent studies demonstrated histopathological correlation between ^{18}F-[FDG] radioactivity and carotid atherosclerotic inflammatory content.[66,69] Observational studies also show that ^{18}F-[FDG] plaque accumulation correlates with the amount of calcified plaques and other cardiovascular risk factors, and interventional drug therapy with statins attenuates ^{18}F-[FDG] atherosclerosis plaque uptake.[70] Moreover, recent gene expression analysis revealed that multiple proteins involved in plaque instability such as CD68, GLUT-1, HK12 and cathepsin K predict ^{18}F-[FDG] uptake in carotid atherosclerotic lesions.[71]

Further studies are also required to demonstrate the relationship between ^{18}F-[FDG] plaque uptake and long-term cardiovascular outcomes. In addition, notable technical and safety limitations need to be addressed in larger prospective studies. For example, there is a possible confounding effect of hyperglycemia in ^{18}F-[FDG] vascular uptake[72] limiting its use in diabetics. Since glucose uptake is a non-specific biomarker of inflammatory activity, other tissues with high ^{18}F-[FDG] metabolic accumulation surrounding the arteries such as fat and skeletal muscle can be a source for false positive results and reduced specificity.

The dose of radiation exposure using co-registration imaging modalities is another technical limitation to consider. There are two sources of radiation exposure during a PET/CT examination: there is an internal radiation exposure from the injected radiopharmaceutical and an external radiation source from the CT scan. The effective radiation exposure for a PET/CT study is the sum of these two sources. A single ^{18}F-[FDG] injection can be the source of 7 millisievert (mSv) effective radiation and the dose of a limited CTA could range from 3 to 15 mSv depending on the acquisition protocol. Even using these conservative estimates of radiation exposure, the combined radiation exposure of a single PET/CT examination is significantly higher than other clinical studies or radiation from natural sources. The average person in the United States receives an effective radiation dose of about 3 mSv from natural sources and cosmic radiation. Thus, during a single PET/CT effective radiation exposure could be comparable to 3–6 years of natural background

radiation exposures. The unknown cumulative and long-term effects of such levels of radiation exposure limit the role of PET/CT in the diagnosis and monitoring of early atherosclerosis until more definitive safety information is collected, particularly in pediatric populations and young adults at risk for cardiovascular disease.[73,74]

Molecular imaging evaluation of arterial thrombosis

Vulnerable plaque rupture invariably leads to platelet activation and aggregation. Activated platelets (AP) adhere to von Willebrand factor (vWF) and other endothelial receptors via glycoprotein (GP) 2αβ1/GPVI receptors.[75] Conformational activation of integrin receptors enhances platelet adhesion to fibrinogen via the GP IIb/IIIa receptor and extracellular matrix collagen through the α2β1 receptor.[76] Pro-coagulant activity is mediated by rearrangement of platelet cell membrane phospholipids (PS). Negatively charged PS activate tenase and prothrombinase activity allowing critical dimensional configuration changes of coagulation factors (IXa, cofactor VIIIa, Xa and Va cofactor) to form initial prothrombotic complexes. Last, AP release dense granules, α-granules and lysosomes with further activation of the coagulation cascade and escalation of the inflammatory response from the denuded endothelium. The end point is the formation of the characteristic 'inflammatory' thrombus by aggregation of platelets and other cellular blood products. In addition to the primary role in thrombosis and hemostasis, it has been hypothesized that AP play a pivotal role in atherogenesis as initiators of a pro-inflammatory response releasing chemokines (ILβ1) and expressing surface receptors (CD40) that facilitate activation of the endothelium, even prior to other initiating events such as lipid retention.[9,10]

The molecular underpinnings of platelet activation have been pursued as potential molecular imaging targets for diverse imaging modalities.[77–80] Annexin V is a 36 kDa protein with special binding affinity for phosphatidylserine in the cell membrane of AP.[81] Annexin V radiolabeled with technectium-99m (^{99m}Tc-Anx) has been used in different animal model systems of acute arterial thrombosis.[78] In addition, ^{99m}Tc-Anx has been used to depict thrombus-related platelets in human valve endocarditis.[82]

Magnetic resonance imaging targeting platelet thrombi also has been achieved with a novel paramagnetic contrast that targets the glycoprotein αII-β3 integrin receptor.[56] Correspondingly, in vivo models of acute arterial thrombosis and in vitro experiments demonstrate that microbubbles targeted to GPIIb/IIIa increase the ultrasonic visualization of human thrombus even under high and pulsatile flow conditions.[83,84]

Imaging-based therapeutic delivery strategies

The general goal of an imaging-based therapeutic delivery system is to visualize and control the delivery of a therapeutic agent to a disease-specific region of interest to improve efficacy while reducing unwanted side effects. The principle is to control drug action in the targeted area by an external energy field such as light, neutron beam, magnetic field or mechanical acoustic energy. Ultrasound in particular has significant advantages to becoming the ideal imaging method to deliver a therapeutic intervention. It is the most commonly used non-invasive diagnostic imaging modality. Ultrasound imaging systems are portable and they provide real-time imaging avoiding hazardous radiation. Moreover, ultrasound is the only non-invasive imaging modality in which multiple human studies demonstrate the feasibility, efficacy and prognostic value of using acoustic energy to facilitate fibrinolysis (thrombus sonolysis) and improve drug delivery into tissues and cells.[85]

Ultrasound-enhanced thrombolysis

Ultrasound waves transmit mechanical and thermal energy in a controllable manner. Based on this principle, dual diagnostic and therapeutic ultrasound strategies are now applied in clinical medicine, including ablation of solid tumors using high-frequency intensity-focused ultrasound (HIFU) and UET to treat acute intra-arterial cerebral ischemia using diagnostic imaging pulses.[86] Clinical trials are underway to evaluate non-invasive UET in the treatment of other acute arterial thrombotic syndromes such as acute myocardial infarction.[87]

Thrombus insonation facilitates fibrinolysis by non-thermal cavitational mechanisms in which the enzymatic activity of tissue plasminogen and other fibrinolytics is enhanced.[88–91] In humans, the use of trans-cranial Doppler (TCD) using high ultrasound frequencies (2 MHz) during tissue plasminogen activator (tPA) infusion is associated with a high rate of arterial recanalization and clinical recovery.[92] The CLOBUST trial (Combined Lysis of Thrombus in Brain Ischemia using Trans-cranial Ultrasound) was the first multicenter collaborative study to demonstrate a positive therapeutic effect in humans of low-dose high-frequency ultrasound. In this study, subjects who received tPA + TCD had a higher rate of arterial recanalization at 2 hours compared to subjects who received tPA infusion alone (38% vs 13%, respectively, $p = 0.03$).[93] More importantly, the rate of intra-cerebral hemorrhage (ICH) was similar in both groups (3.8%, p = NS).[94] A recently published meta-analysis of six randomized and three non-randomized studies, pooling a total of 416 participants, confirmed the safety and efficacy of high-frequency UET. The group that received UET had a significantly higher likelihood of recanalization (odds ratio [OR], 2.99, $p = 0.0001$), whereas no associated risk of symptomatic ICH was observed (pooled OR, 1.26, $p = 0.67$).[95]

Acoustic and magnetic active probes as therapeutic carrier systems

Ultrasound by itself facilitates the therapeutic effect and cellular uptake of drugs, proteins, peptides and even gene and cell therapies. However, the amount of ultrasound energy required to induce such site-specific effects in a controllable manner could be deleterious to surrounding tissues.[96] Thus, microbubbles have been used to decrease acoustic energy to achieve a therapeutic effect and as therapeutic carriers to the region of interest. During acoustic stimulus they tend to release energy from their implosive collapse and growth within vasculature (nuclei cavitation). This release of energy can induce cell membrane sonoporation, facilitating the delivery of a loaded therapeutic agent.[97,98]

Multiple proof-of-principle studies demonstrate the feasibility of using acoustically active probes as carriers for drugs and gene therapies. Glycoprotein IIb/IIIa targeted microbubbles improve microvascular flow after acute coronary obstruction in a large animal model system.[99] In angiogenesis, ultrasound-mediated delivery of a VEGF plasmid in the hind limb ischemia model was superior to direct intra-muscular delivery in promoting neovascular formation.[100,101] Recently, effective transfection into arteries was demonstrated using microbubbles carrying ICAM-1 small interfering RNA (siRNA). In this study, ICAM-1 siRNA attenuated arterial neointimal formation.[102] The development of imaging systems specifically designed for ultrasound therapeutic delivery and development of novel UCAs at the nanoscale will further increase the specificity of an ultrasound-based theragnostic approach.[103]

Based on similar principles, magnetic drug targeting (MDT) is a novel theragnostic approach for site-specific vascular intervention. An external magnetic field is used to attract and activate metallic nano particles (MNP) made of iron, cobalt or nickel, whereas protective polymeric coating, liposomes or another alternative core shell structure coating are used for drug loading and tagging with a functional ligand to further increase molecular

specificity.[104] Novel co-registration technology that uses an MRI-guided focused ultrasound system (MRIgFUS) is currently under development. MRI provides a precise anatomic localization and structural assessment of the target vessel, whereas focused high-frequency ultrasound is used to deliver drug-loaded and tagged probes to deep vascular targets.[105]

Summary

Molecular imaging applications designed for imaging platforms traditionally used to evaluate cardiovascular disease have a complementary role in depicting molecular characteristics of the heterogeneous atherosclerotic process. Iron oxide superparamagnetic particles for MRI and ^{18}F-[FDG] for PET/CT are well-developed molecular imaging tools to monitor atherosclerotic plaque inflammation. Similarly, contrast-enhanced ultrasound appears to be a reliable real-time method to depict ectopic neovascularization in humans. Evidence from early phase interventional drug trials in humans suggests a probable role of these molecular imaging applications in clinical practice.

Clinical studies using UET applications in acute cerebral ischemia and acute coronary syndrome are compelling examples that a theragnostic approach to vascular disease is feasible in humans. Furthermore, based on successful pre-clinical studies in animal model systems that use acoustically and magnetically active probes to deliver drug, gene or cellular-based therapies, it is reasonable to expect in the near future a human translation of novel molecular theragnostic applications that comprehensibly account for the structural, functional, and pathobiologic characteristics of the disease. This approach may eventually lead to a specific and personalized treatment of atherosclerosis and other vascular conditions.

Acknowledgments

Luis H Eraso, MD is supported by a NHLBI-K12 Career Development Award (K12-HL083772, PI: Emile Mohler III, MD).

References

1. Herschman HR. Molecular imaging: looking at problems, seeing solutions. Science. 2003; 302:605–608. [PubMed: 14576425]
2. Ozdemir V, Williams-Jones B, Glatt SJ, Tsuang MT, Lohr JB, Reist C. Shifting emphasis from pharmacogenomics to theragnostics. Nat Biotechnol. 2006; 24:942–946. [PubMed: 16900136]
3. McCarthy JR, Weissleder R. Multifunctional magnetic nanoparticles for targeted imaging and therapy. Adv Drug Deliv Rev. 2008; 60:1241–1251. [PubMed: 18508157]
4. Laing ST, McPherson DD. Cardiovascular therapeutic uses of targeted ultrasound contrast agents. Cardiovasc Res. 2009; 83:626–635. [PubMed: 19581314]
5. Williams KJ, Tabas I. The response-to-retention hypothesis of early atherogenesis. Arterioscler Thromb Vasc Biol. 1995; 15:551–561. [PubMed: 7749869]
6. Tabas I, Williams KJ, Boren J. Subendothelial lipoprotein retention as the initiating process in atherosclerosis: update and therapeutic implications. Circulation. 2007; 116:1832–1844. [PubMed: 17938300]
7. Hansson GK. Inflammation, atherosclerosis, and coronary artery disease. N Engl J Med. 2005; 352:1685–1695. [PubMed: 15843671]
8. Cybulsky MI, Gimbrone MA Jr. Endothelial expression of a mononuclear leukocyte adhesion molecule during athero-genesis. Science. 1991; 251:788–791. [PubMed: 1990440]
9. Massberg S, Brand K, Gruner S, et al. A critical role of platelet adhesion in the initiation of atherosclerotic lesion formation. J Exp Med. 2002; 196:887–896. [PubMed: 12370251]
10. May AE, Seizer P, Gawaz M. Platelets: inflammatory firebugs of vascular walls. Arterioscler Thromb Vasc Biol. 2008; 28:s5–s10. [PubMed: 18174454]

11. Boring L, Gosling J, Cleary M, Charo IF. Decreased lesion formation in CCR2−/− mice reveals a role for chemokines in the initiation of atherosclerosis. Nature. 1998; 394:894–897. [PubMed: 9732872]
12. Li AC, Glass CK. The macrophage foam cell as a target for therapeutic intervention. Nat Med. 2002; 8:1235–1242. [PubMed: 12411950]
13. Den Dekker WK, Cheng C, Pasterkamp G, Duckers HJ. Toll like receptor 4 in atherosclerosis and plaque destabilization. Atherosclerosis. 2010; 2:314–320. [PubMed: 19900676]
14. Linton MF, Fazio S. Class A scavenger receptors, macrophages, and atherosclerosis. Curr Opin Lipidol. 2001; 12:489–495. [PubMed: 11561167]
15. Virmani R, Burke AP, Farb A, Kolodgie FD. Pathology of the unstable plaque. Prog Cardiovasc Dis. 2002; 44:349–356. [PubMed: 12024333]
16. Whatling C, Bjork H, Gredmark S, Hamsten A, Eriksson P. Effect of macrophage differentiation and exposure to mildly oxidized LDL on the proteolytic repertoire of THP-1 monocytes. J Lipid Res. 2004; 45:1768–1776. [PubMed: 15210849]
17. Volcik KA, Campbell S, Chambless LE, et al. MMP2 genetic variation is associated with measures of fibrous cap thickness: The Atherosclerosis Risk in Communities Carotid MRI Study. Atherosclerosis. 2010; 210:188–193. [PubMed: 20064641]
18. Feinstein SB. Contrast ultrasound imaging of the carotid artery vasa vasorum and atherosclerotic plaque neovascularization. J Am Coll Cardiol. 2006; 48:236–243. [PubMed: 16843169]
19. Kaufmann BA, Sanders JM, Davis C, et al. Molecular imaging of inflammation in atherosclerosis with targeted ultrasound detection of vascular cell adhesion molecule-1. Circulation. 2007; 116:276–284. [PubMed: 17592078]
20. Gramiak R, Shah PM. Echocardiography of the aortic root. Invest Radiol. 1968; 3:356–366. [PubMed: 5688346]
21. Lindner JR, Song J, Jayaweera AR, Sklenar J, Kaul S. Microvascular rheology of Definity microbubbles after intra-arterial and intravenous administration. J Am Soc Echocardiogr. 2002; 15:396–403. [PubMed: 12019422]
22. Villanueva FS. Molecular imaging of cardiovascular disease using ultrasound. J Nucl Cardiol. 2008; 15:576–586. [PubMed: 18674725]
23. Kaufmann BA, Lindner JR. Molecular imaging with targeted contrast ultrasound. Curr Opin Biotech. 2007; 18:11–16. [PubMed: 17241779]
24. Xiong L, Deng YB, Zhu Y, Liu YN, Bi XJ. Correlation of carotid plaque neovascularization detected by using contrast-enhanced US with clinical symptoms. Radiology. 2009; 251:583–589. [PubMed: 19304920]
25. Kalantarinia K, Belcik JT, Patrie JT, Wei K. Real-time measurement of renal blood flow in healthy subjects using contrast-enhanced ultrasound. Am J Physiol Renal Physiol. 2009; 297:F1129–F1134. [PubMed: 19625375]
26. Duerschmied D, Olson L, Olschewski M, et al. Contrast ultrasound perfusion imaging of lower extremities in peripheral arterial disease: a novel diagnostic method. Eur Heart J. 2006; 27:310–315. [PubMed: 16308326]
27. Porter TR, Xie F, Silver M, Kricsfeld D, O'Leary E. Real-time perfusion imaging with low mechanical index pulse inversion Doppler imaging. J Am Coll Cardiol. 2001; 37:748–753. [PubMed: 11693747]
28. Stride E. Physical principles of microbubbles for ultrasound imaging and therapy. Cerebrovasc Dis. 2009; 27(suppl 2):1–13. [PubMed: 19372656]
29. Voigt JU. Ultrasound molecular imaging. Methods. 2009; 48:92–97. [PubMed: 19324089]
30. Miller DL, Averkiou MA, Brayman AA, et al. Bioeffects considerations for diagnostic ultrasound contrast agents. J Ultrasound Med. 2008; 27:611–632. [PubMed: 18359911]
31. Kurt M, Shaikh KA, Peterson L, et al. Impact of contrast echocardiography on evaluation of ventricular function and clinical management in a large prospective cohort. J Am Coll Cardiol. 2009; 53:802–810. [PubMed: 19245974]
32. Wei K, Mulvagh SL, Carson L, et al. The safety of deFinity and Optison for ultrasound image enhancement: a retrospective analysis of 78,383 administered contrast doses. J Am Soc Echocardiogr. 2008; 21:1202–1206. [PubMed: 18848430]

33. Abdelmoneim SS, Bernier M, Scott CG, et al. Safety of contrast agent use during stress echocardiography: a 4-year experience from a single-center cohort study of 26,774 patients. JACC Cardiovasc Imaging. 2009; 2:1048–1056. [PubMed: 19761981]
34. Weyman AE. The year in echocardiography. J Am Coll Cardiol. 2009; 53:1558–1567. [PubMed: 19389569]
35. Keske MA, Clerk LH, Price WJ, Jahn LA, Barrett EJ. Obesity blunts microvascular recruitment in human forearm muscle after a mixed meal. Diabetes Care. 2009; 32:1672–1677. [PubMed: 19487636]
36. Womack L, Peters D, Barrett EJ, Kaul S, Price W, Lindner JR. Abnormal skeletal muscle capillary recruitment during exercise in patients with type 2 diabetes mellitus and microvascular complications. J Am Coll Cardiol. 2009; 53:2175–2183. [PubMed: 19497445]
37. Fleiner M, Kummer M, Mirlacher M, et al. Arterial neovascularization and inflammation in vulnerable patients: early and late signs of symptomatic atherosclerosis. Circulation. 2004; 110:2843–2850. [PubMed: 15505090]
38. Staub D, Schinkel AF, Coll B, et al. Contrast-enhanced ultrasound imaging of the vasa vasorum: from early atherosclerosis to the identification of unstable plaques. JACC Cardiovasc Imaging. 2010; 3:761–771. [PubMed: 20633855]
39. Vela D, Buja LM, Madjid M, et al. The role of periadventitial fat in atherosclerosis. Arch Pathol Lab Med. 2007; 131:481–487. [PubMed: 17516753]
40. Herrmann J, Lerman LO, Rodriguez-Porcel M, et al. Coronary vasa vasorum neovascularization precedes epicardial endothelial dysfunction in experimental hypercholesterolemia. Cardiovasc Res. 2001; 51:762–766. [PubMed: 11530109]
41. Sluimer JC, Gasc JM, van Wanroij JL, et al. Hypoxia, hypoxia-inducible transcription factor, and macrophages in human atherosclerotic plaques are correlated with intraplaque angiogenesis. J Am Coll Cardiol. 2008; 51:1258–1265. [PubMed: 18371555]
42. Schinkel AF, Krueger CG, Tellez A, et al. Contrast-enhanced ultrasound for imaging vasa vasorum: comparison with histopathology in a swine model of atherosclerosis. Eur J Echocardiogr. 2010; 11:659–664. [PubMed: 20385655]
43. Vicenzini E, Giannoni MF, Puccinelli F, et al. Detection of carotid adventitial vasa vasorum and plaque vascularization with ultrasound cadence contrast pulse sequencing technique and echo-contrast agent. Stroke. 2007; 38:2841–2843. [PubMed: 17761913]
44. Giannoni MF, Vicenzini E, Citone M, et al. Contrast carotid ultrasound for the detection of unstable plaques with neoangiogenesis: a pilot study. Eur J Vasc Endovasc Surg. 2009; 37:722–727. [PubMed: 19328729]
45. Magnoni M, Coli S, Marrocco-Trischitta MM, et al. Contrast-enhanced ultrasound imaging of periadventitial vasa vasorum in human carotid arteries. Eur J Echocardiogr. 2009; 10:260–264. [PubMed: 18757860]
46. Shah F, Balan P, Weinberg M, et al. Contrast-enhanced ultrasound imaging of atherosclerotic carotid plaque neovascularization: a new surrogate marker of atherosclerosis? Vasc Med. 2007; 12:291–297. [PubMed: 18048465]
47. Lindner JR. Contrast ultrasound molecular imaging of inflammation in cardiovascular disease. Cardiovasc Res. 2009; 84:182–189. [PubMed: 19783842]
48. Fisher NG, Christiansen JP, Klibanov A, Taylor RP, Kaul S, Lindner JR. Influence of microbubble surface charge on capillary transit and myocardial contrast enhancement. J Am Coll Cardiol. 2002; 40:811–819. [PubMed: 12204515]
49. Tsutsui JM, Xie F, Cano M, et al. Detection of retained microbubbles in carotid arteries with real-time low mechanical index imaging in the setting of endothelial dysfunction. J Am Coll Cardiol. 2004; 44:1036–1046. [PubMed: 15337216]
50. Kaufmann BA, Carr CL, Belcik JT, et al. Molecular imaging of the initial inflammatory response in atherosclerosis: implications for early detection of disease. Arterioscler Thromb Vasc Biol. 2010; 30:54–59. [PubMed: 19834105]
51. Hamilton AJ, Huang S-L, Warnick D, et al. Intravascular ultrasound molecular imaging of atheroma components in vivo. J Am Coll Cardiol. 2004; 43:453–460. [PubMed: 15013130]

52. Kooi ME, Cappendijk VC, Cleutjens KBJM, et al. Accumulation of ultrasmall superparamagnetic particles of iron oxide in human atherosclerotic plaques can be detected by in vivo magnetic resonance imaging. Circulation. 2003; 107:2453–2458. [PubMed: 12719280]
53. Trivedi RA, Mallawarachi C, U-King-Im JM, et al. Identifying inflamed carotid plaques using in vivo USPIO-enhanced MR imaging to label plaque macrophages. Arterioscler Thromb Vasc Biol. 2006; 26:1601–1606. [PubMed: 16627809]
54. Tang TY, Howarth SPS, Miller SR, et al. The ATHEROMA (Atorvastatin Therapy: Effects on Reduction of Macrophage Activity) Study: evaluation using ultrasmall superparamagnetic iron oxide-enhanced magnetic resonance imaging in carotid disease. J Am Coll Cardiol. 2009; 53:2039–2050. [PubMed: 19477353]
55. Tang TY, Muller KH, Graves MJ, et al. Iron oxide particles for atheroma imaging. Arterioscler Thromb Vasc Biol. 2009; 29:1001–1008. [PubMed: 19229073]
56. Von zur Muhlen C, von Elverfeldt D, Bassler N, et al. Superparamagnetic iron oxide binding and uptake as imaged by magnetic resonance is mediated by the integrin receptor Mac-1 (CD11b/CD18): implications on imaging of atherosclerotic plaques. Atherosclerosis. 2007; 193:102–111. [PubMed: 16997307]
57. Nicolau B, Catherine C, Anna Louise B, et al. In vivo visualization of macrophage infiltration and activity in inflammation using magnetic resonance imaging. Wiley Interdisciplinary Reviews: Nanomedicine and Nanobiotechnology. 2009; 1:272–298. [PubMed: 20049797]
58. Sullivan JL. Macrophage iron, hepcidin, and atherosclerotic plaque stability. Exp Biol Med. 2007; 232:1014–1020.
59. Stadler N, Lindner RA, Davies MJ. Direct detection and quantification of transition metal ions in human atherosclerotic plaques: evidence for the presence of elevated levels of iron and copper. Arterioscler Thromb Vasc Biol. 2004; 24:949–954. [PubMed: 15001454]
60. David PC, Karen CB-S, Willem JMM, et al. An ApoA-I mimetic peptide high-density-lipoprotein-based MRI contrast agent for atherosclerotic plaque composition detection. Small. 2008; 4:1437–1444. [PubMed: 18712752]
61. Briley-Saebo KC, Shaw PX, Mulder WJM, et al. Targeted molecular probes for imaging atherosclerotic lesions with magnetic resonance using antibodies that recognize oxidation-specific epitopes. Circulation. 2008; 117:3206–3215. [PubMed: 18541740]
62. Townsend D, Cherry S. Combining anatomy and function: the path to true image fusion. Eur Radiol. 2001; 11:1968–1974. [PubMed: 11702130]
63. Alexanderson E, Slomka P, Cheng V, et al. Fusion of positron emission tomography and coronary computed tomographic angiography identifies fluorine 18 fluorodeoxyglucose uptake in the left main coronary artery soft plaque. J Nucl Cardiol. 2008; 15:841–843. [PubMed: 18984461]
64. Libby P. Inflammation in atherosclerosis. Nature. 2002; 420:868–874. [PubMed: 12490960]
65. Ogawa M, Ishino S, Mukai T, et al. 18F-FDG Accumulation in atherosclerotic plaques: immunohistochemical and PET imaging study. J Nucl Med. 2004; 45:1245–1250. [PubMed: 15235073]
66. Rudd JHF, Warburton EA, Fryer TD, et al. Imaging atherosclerotic plaque inflammation with [18F]-fluorodeoxyglucose positron emission tomography. Circulation. 2002; 105:2708–2711. [PubMed: 12057982]
67. Zhang Z, Machac J, Helft G, et al. Non-invasive imaging of atherosclerotic plaque macrophage in a rabbit model with F-18 FDG PET: a histopathological correlation. BMC Nucl Med. 2006; 6:3. [PubMed: 16725052]
68. Yun M, Yeh D, Araujo LI, Jang S, Newberg A, Alavi A. F-18 FDG uptake in the large arteries: a new observation. Clin Nucl Med. 2001; 26:314–319. [PubMed: 11290891]
69. Tawakol A, Migrino RQ, Bashian GG, et al. In vivo 18F-fluorodeoxyglucose positron emission tomography imaging provides a noninvasive measure of carotid plaque inflammation in patients. J Am Coll Cardiol. 2006; 48:1818–1824. [PubMed: 17084256]
70. Tahara N, Kai H, Ishibashi M, et al. Simvastatin attenuates plaque inflammation: evaluation by fluorodeoxyglucose positron emission tomography. J Am Coll Cardiol. 2006; 48:1825–1831. [PubMed: 17084257]

71. Pedersen SF, Graebe M, Fisker Hag AM, Hojgaard L, Sillesen H, Kjaer A. Gene expression and 18FDG uptake in atherosclerotic carotid plaques. Nucl Med Commun. 2010; 31:423–429. [PubMed: 20145577]
72. Zhao S, Kuge Y, Tsukamoto E, et al. Effects of insulin and glucose loading on FDG uptake in experimental malignant tumours and inflammatory lesions. Eur J Nucl Med. 2001; 28:730. [PubMed: 11440033]
73. Devine CE, Mawlawi O. Radiation safety with positron emission tomography and computed tomography. Semin Ultrasound CT MR. 2010; 31:39–45. [PubMed: 20102694]
74. Brenner DJ, Hall EJ. Computed tomography—an increasing source of radiation exposure. N Engl J Med. 2007; 357:2277–2284. [PubMed: 18046031]
75. Nieswandt B, Watson SP. Platelet-collagen interaction: is GPVI the central receptor? Blood. 2003; 102:449–461. [PubMed: 12649139]
76. Mazzucato M, Cozzi MR, Battiston M, et al. Distinct spatio-temporal Ca^{2+} signaling elicited by integrin {alpha}2{beta}1 and glycoprotein VI under flow. Blood. 2009; 114:2793–2801. [PubMed: 19622836]
77. Klink A, Lancelot E, Ballet S, et al. Magnetic resonance molecular imaging of thrombosis in an arachidonic acid mouse model using an activated platelet targeted probe. Arterioscler Thromb Vasc Biol. 2010; 30:403–410. [PubMed: 20139362]
78. Tait JF, Cerqueira MD, Dewhurst TA, Fujikawa K, Ritchie JL, Stratton JR. Evaluation of annexin V as a platelet-directed thrombus targeting agent. Thromb Res. 1994; 75:491–501. [PubMed: 7992250]
79. Von zur Muhlen C, Peter K, Ali ZA, et al. Visualization of activated platelets by targeted magnetic resonance imaging utilizing conformation-specific antibodies against glycoprotein IIb/IIIa. J Vasc Res. 2009; 46:6–14. [PubMed: 18515970]
80. Schumann PAB, Christiansen JPCM, Quigley RMB, et al. Targeted-microbubble binding selectively to GPIIb IIIa receptors of platelet thrombi. Invest Radiol. 2002; 37:587–593. [PubMed: 12393970]
81. Thiagarajan P, Tait JF. Binding of annexin V/placental anticoagulant protein I to platelets Evidence for phosphatidyl-serine exposure in the procoagulant response of activated platelets. J Biol Chem. 1990; 265 17,420–17,423.
82. Kietselaer BLJH, Narula J, Hofstra L. The Annexin code: revealing endocarditis. Eur Heart J. 2007; 28:948. [PubMed: 17085485]
83. Alonso A, Della Martina A, Stroick M, et al. Molecular imaging of human thrombus with novel abciximab immunobubbles and ultrasound. Stroke. 2007; 38:1508–1514. [PubMed: 17379828]
84. Martin MJ, Chung EML, Goodall AH, et al. Enhanced detection of thromboemboli with the use of targeted microbubbles. Stroke. 2007; 38:2726–2732. [PubMed: 17823379]
85. Rao R, Nanda S. Sonophoresis: recent advancements and future trends. J Pharm Pharmacol. 2009; 61:689–705. [PubMed: 19505359]
86. Alexandrov AV. Ultrasound-enhanced thrombolysis for stroke: clinical significance. Eur J Ultrasound. 2002; 16:131–140. [PubMed: 12470858]
87. Slikkerveer J, Dijkmans P, Sieswerda G, et al. Ultrasound enhanced prehospital thrombolysis using microbubbles infusion in patients with acute ST elevation myocardial infarction: rationale and design of the Sonolysis study. Trials. 2008; 9:72. [PubMed: 19068143]
88. Bookstein JJ, Saldinger E. Accelerated thrombolysis: in vitro evaluation of agents and methods of administration. Invest Radiol. 1985; 20:731–735. [PubMed: 2933363]
89. Francis CW, Blinc A, Lee S, Cox C. Ultrasound accelerates transport of recombinant tissue plasminogen activator into clots. Ultrasound Med Biol. 1995; 21:419–424. [PubMed: 7645133]
90. Sehgal CM, Leveen RF, Shlansky-Goldberg RD. Ultrasound-assisted thrombolysis. Invest Radiol. 1993; 28:939–943. [PubMed: 8262749]
91. Shlansky-Goldberg RD, Cines DB, Sehgal CM. Catheter-delivered ultrasound potentiates in vitro thrombolysis. J Vasc Interv Radiol. 1996; 7:313–320. [PubMed: 8761806]
92. Alexandrov AV, Demchuk AM, Felberg RA, et al. High rate of complete recanalization and dramatic clinical recovery during tPA infusion when continuously monitored with 2-MHz transcranial Doppler monitoring. Stroke. 2000; 31:610–614. [PubMed: 10700493]

93. Alexandrov AV, Molina CA, Grotta JC, et al. Ultrasound-enhanced systemic thrombolysis for acute ischemic stroke. N Engl J Med. 2004; 351:2170–2178. [PubMed: 15548777]

94. Alexandrov AV. Ultrasound enhancement of fibrinolysis. Stroke. 2009; 40(3 suppl 1):S107–S110. [PubMed: 19064806]

95. Tsivgoulis G, Eggers J, Ribo M, et al. Safety and efficacy of ultrasound-enhanced thrombolysis: a comprehensive review and meta-analysis of randomized and nonrandomized studies. Stroke. 2010; 41:280–287. [PubMed: 20044531]

96. Mayer CR, Bekeredjian R. Ultrasonic gene and drug delivery to the cardiovascular system. Adv Drug Deliv Rev. 2008; 60:1177–1192. [PubMed: 18474407]

97. Laing ST, McPherson DD. Cardiovascular therapeutic uses of targeted ultrasound contrast agents. Cardiovasc Res. 2009; 83:626–635. [PubMed: 19581314]

98. Tachibana K, Tachibana S. Albumin microbubble echocontrast material as an enhancer for ultrasound accelerated thrombolysis. Circulation. 1995; 92:1148–1150. [PubMed: 7648659]

99. Xie F, Lof J, Matsunaga T, Zutshi R, Porter TR. Diagnostic ultrasound combined with glycoprotein IIb/IIIa-targeted microbubbles improves microvascular recovery after acute coronary thrombotic occlusions. Circulation. 2009; 119:1378–1385. [PubMed: 19255341]

100. Leong-Poi H, Kuliszewski MA, Lekas M, et al. Therapeutic arteriogenesis by ultrasound-mediated VEGF165 plasmid gene delivery to chronically ischemic skeletal muscle. Circ Res. 2007; 101:295–303. [PubMed: 17585071]

101. Kobulnik J, Kuliszewski MA, Stewart DJ, Lindner JR, Leong-Poi H. Comparison of gene delivery techniques for therapeutic angiogenesis: ultrasound-mediated destruction of carrier microbubbles versus direct intramuscular injection. J Am Coll Cardiol. 2009; 54:1735–1742. [PubMed: 19850216]

102. Suzuki J, Ogawa M, Takayama K, et al. Ultrasound-microbubble-mediated intercellular adhesion molecule-1 small interfering ribonucleic acid transfection attenuates neointimal formation after arterial injury in mice. J Am Coll Cardiol. 2010; 55:904–913. [PubMed: 20185042]

103. Seip R, Chien Ting C, Hall CS, Raju BI, Ghanem A, Tiemann K. Targeted ultrasound-mediated delivery of nanoparticles: on the development of a new HIFU-based therapy and imaging device. IEEE Trans Biomed Eng. 2009; 57:61–70. [PubMed: 19695986]

104. Sun C, Lee JSH, Zhang M. Magnetic nanoparticles in MR imaging and drug delivery. Adv Drug Deliv Rev. 2008; 60:1252–1265. [PubMed: 18558452]

105. Hynynen K. MRI-guided focused ultrasound treatments. Ultrasonics. 2009; 50:221–229. [PubMed: 19818981]

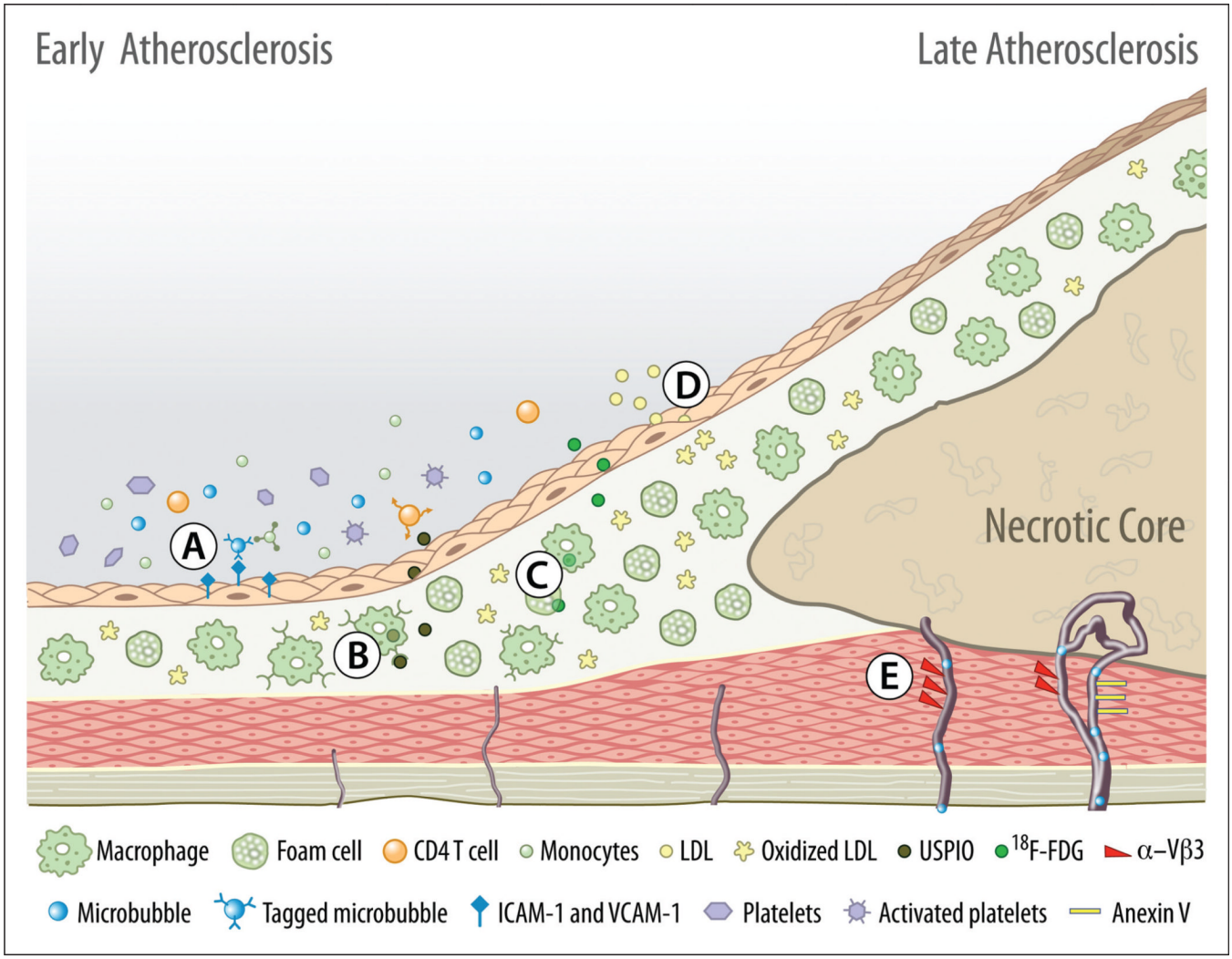

Figure 1.

Multimodal atherosclerosis molecular imaging. Depicted targets represent molecular imaging applications designed for platforms currently used in clinical medicine such as ultrasound, MRI or PET/SPECT/CT imaging. (A) Endothelial activation and immune cell activity assessment by microbubbles tagged with ICAM-1 / VCAM-1 antibodies. (B) Atherosclerosis plaque inflammatory activity imaging with MRI using ultra-small superparamagnetic particles of iron oxide (USPIO) which have an increased affinity for the activated macrophage scavenger receptors. (C) Activated macrophage and foam cells increased metabolic activity imaging with ^{18}F-[FDG] (fluoro-2-deoxy-D-glucose) uptake. (D) Oxidized low-density lipoprotein (ox-LDL) analogs using MRI. (E) Plaque neovascularization assessment with non-tagged microbubbles and tagged (Vβ3, annexin V) microbubbles, and other nanoparticles designed for MRI and PET/CT.

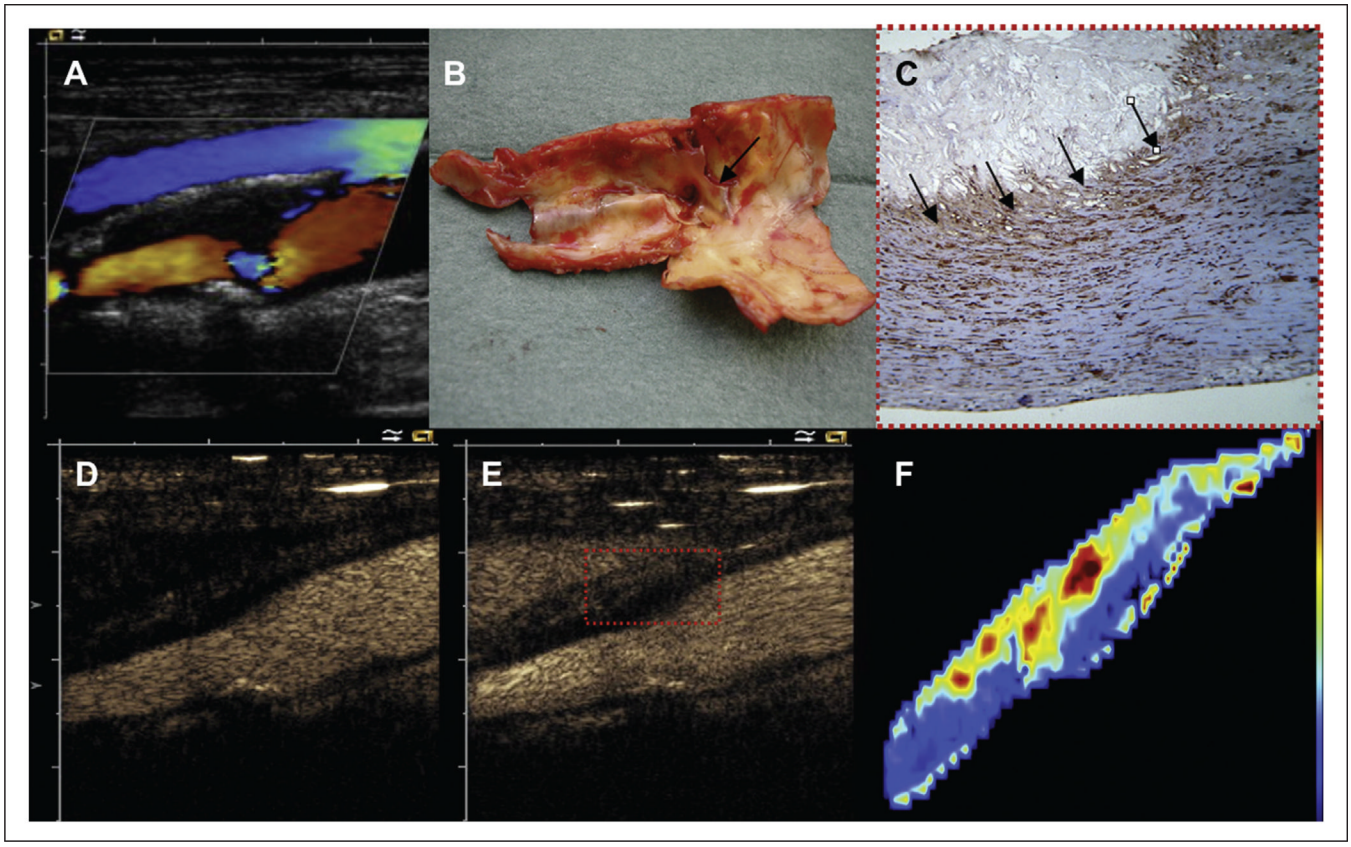

Figure 2.
Contrast-enhanced ultrasound assessment of unstable plaque neovascularization. Carotid artery duplex scan and pathologic findings of a patient with acute symptomatic cerebrovascular disease. (A) Non-enhanced color Doppler image representing a heterogeneous, mainly hypoechoic, with a proximal posterior hyperechoic, calcified area, and severe carotid stenosis. (B) Gross pathological findings from surgical endarterectomy showing a hemorrhagic plaque. (C) Immunohistological staining for VEGF (20×) shows diffuse staining, with multiple small microvessels (20–30 μm diameter; arrows). (D) and (E, rectangle) show high diffuse contrast enhancement consistent with vascularization at the base of the lesion. (F) Qontrast software imaging analysis of the distribution of plaque vascularization. Reprinted from ref. 44, copyright 2009, with permission from Elsevier.

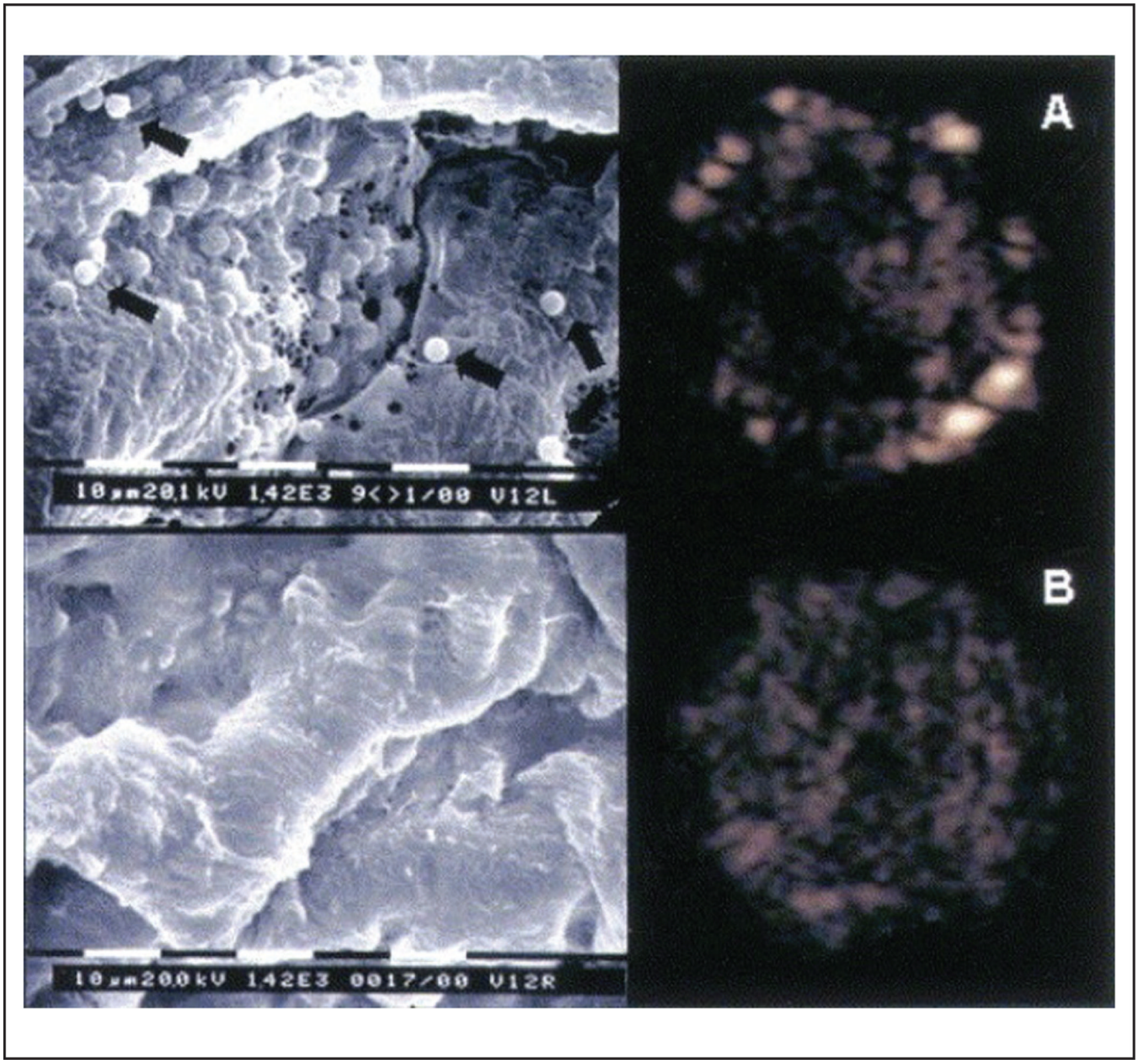

Figure 3.

Microbubble retention by activated endothelium in the carotid arteries. High magnification (bar = 10 μm; magnification 1420×) scanning electron microscopy pictures (left panels) and their respective low mechanical index pulse sequence scheme (PSS) images (right panels). Panel A demonstrates the presence of retained microbubbles in the endothelium detected by PSS in the left injured carotid artery, and panel B reveals the absence of microbubbles in the endothelium in the control right side. Scanning electron microscopy revealed sites of injury with endothelial denudation and attachment of microbubbles (black arrows) to the denuded endothelium only in the injured vessel (A) and normal-appearing endothelium in the control vessel (B). Reprinted from ref. 49, copyright 2004, with permission from Elsevier.

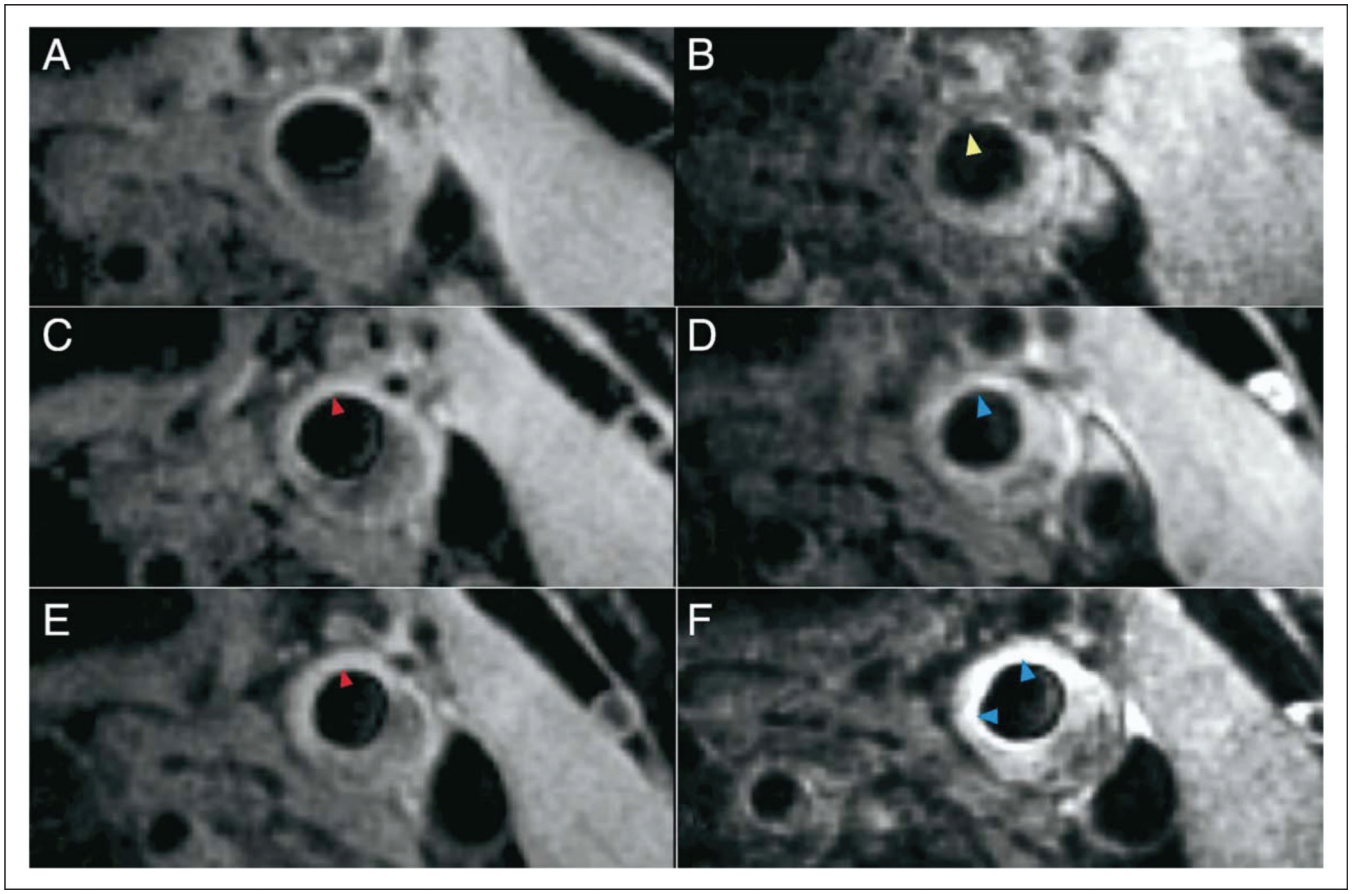

Figure 4.

Super-magnetic iron oxide uptake by atherosclerosis plaque. Example of high-dose patient T2*-weighted imaging of a left common carotid artery before and after ultra-small superparamagnetic iron oxide (USPIO) infusion at the three time points of (A and B) 0, (C and D) 6, and (E and F) 12 weeks. (B) USPIO uptake can clearly be seen in the plaque at baseline (yellow arrowhead). (C and E) Pre-USPIO imaging remains very similar at all three time points with Sinerem having been cycled out of the plaque before re-imaging (red arrowhead). (D) The plaque begins to enhance at 6 weeks (blue arrowhead). This signifies that there is a predominant T1 effect, indicating minimal USPIO uptake and a lack of activated macrophages (minimal inflammation). (E) No residual USPIO signal is also seen in the pre-USPIO imaging at 12 weeks, and (F) signal enhancement post-USPIO can be seen with no evidence of signal voids (blue arrowheads). Reprinted from ref. 54, copyright 2009, with permission from Elsevier.

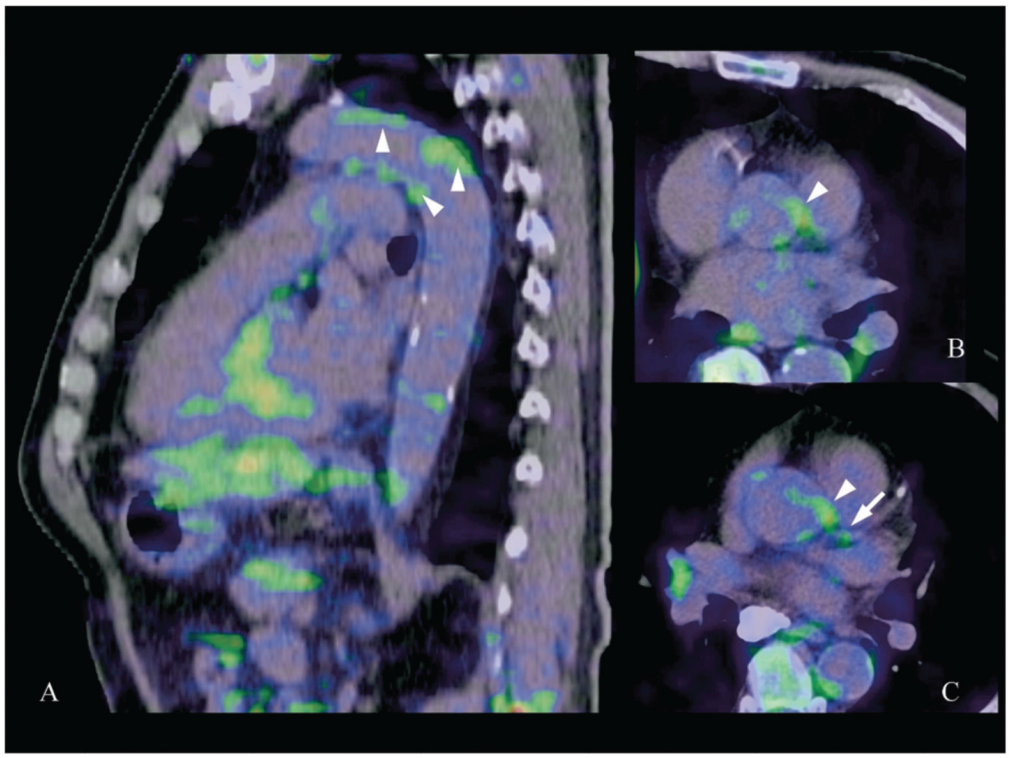

Figure 5.
^{18}F-[FDG] uptake from non-calcified inflammatory aortic and coronary plaques. ^{18}F-[FDG] PET/CT fusion image with evidence of inflammatory signaling from the corresponding left main coronary (arrow) and aortic atherosclerotic plaques (arrowheads). With kind permission from Springer Science+Business Media: ref. 63.